Journal of the Optical Society of America B

Theory of four-wave mixing of cylindrical vector beams in optical fibers

E. Scott Goudreau,[1] Connor Kupchak,[1,2,3] Benjamin J. Sussman,[1,3,4] Robert W. Boyd,[1,5] and Jeff S. Lundeen[1,3,*]

[1]*Department of Physics, Centre for Research in Photonics, University of Ottawa, 25 Templeton St, Ottawa, Ontario K1N 6N5, Canada*
[2]*Department of Electronics, Carleton University, 1125 Colonel By Dr, Ottawa, Ontario K1S 5B6, Canada*
[3]*Joint Centre for Extreme Photonics, Ottawa, Ontario K1N 0R6, Canada*
[4]*National Research Council of Canada, 100 Sussex Dr, Ottawa, Ontario K1N 0R6, Canada*
[5]*The Institute of Optics and Department of Physics and Astronomy, University of Rochester, Rochester, New York 14627, USA*
Corresponding author: jlundeen@uottawa.ca

Cylindrical vector (CV) beams are a set of transverse spatial modes that exhibit a cylindrically symmetric intensity profile and a variable polarization about the beam axis. They are composed of a non-separable superposition of orbital and spin angular momenta. Critically, CV beams are also the eigenmodes of optical fiber and, as such, are of widespread practical importance in photonics and have the potential to increase communications bandwidth through spatial multiplexing. Here, we derive the coupled amplitude equations that describe the four-wave mixing (FWM) of CV beams in optical fibers. These equations allow us to determine the selection rules that govern the interconversion of CV modes in FWM processes. With these selection rules, we show that FWM conserves the total angular momentum, the sum of orbital and spin angular momenta, in the conversion of two input photons to two output photons. When applied to spontaneous FWM, the selection rules show that photon pairs can be generated in CV modes directly and can be entangled in those modes. Such quantum states of light in CV modes could benefit technologies such as quantum key distribution with satellites. © 2020 Optical Society of America

https://doi.org/10.1364/JOSAB.386622

1. INTRODUCTION

The term "structured light" refers to optical beams whose intensity, phase, or polarization are non-uniform across the beam's transverse profile. Cylindrical vector (CV) beams are a type of structured light that exhibits intensity and polarization profiles that are spatially dependent but also exhibit symmetry under discrete rotations about the beam axis. Specifically, the modes for such structured light beams, CV modes, are described by a superposition of product states between the spin angular momentum (SAM) and orbital angular momentum (OAM) degrees of freedom. Utilizing the degrees of freedom available in the transverse profile of an optical beam can benefit many applications. These can include more complex mode-division multiplexing techniques to increase communications bandwidth. Such multiplexing techniques have already been demonstrated with scalar OAM modes [1,2] and vector beam modes [3,4]. Similarly, from a quantum optics viewpoint, CV modes can increase the information capacity available in single photons via the additional OAM and SAM degrees of freedom. In free-space quantum key distribution, the rotational symmetry of CV modes can be exploited to alleviate the need for

rotational alignment between sending and receiving parties [5]. Outside of communications, the behavior of optical beams in CV modes are of fundamental interest. For example, radially polarized modes focus to smaller spot sizes than Gaussian modes of a comparable beam waist [6], and azimuthally polarized modes produce a longitudinal magnetic field at their focus.

Thorough understanding of nonlinear optical processes is vital to many practical applications. An example is telecommunications, where unwanted nonlinear interactions between optical pulses in fiber present a roadblock for increasing signal power, and thus the bandwidth [7]. To date, the theory for four-wave mixing (FWM) in fiber systems has been developed for both uniformly polarized light [8,9] and spatial modes [10–12]. Despite their potential for increasing communications bandwidth, the nonlinear optics of structured light and vector modes is in its infancy [13–15]. In order to address this, here we derive the coupled amplitude equations that describe FWM of CV and other complex modes. Using this, we derive a set of general selection rules for the allowed mixing processes between CV modes. FWM processes can convert photons between different CV modes and may provide insight into conversion

processes that involve structured light and the conservation of angular momentum of light. Moreover, these FWM transitions can potentially produce mode-entangled CV photons through spontaneous FWM (SFWM) photon pair generation.

2. OPTICAL MODE DESCRIPTIONS

We begin with a review of optical spatial modes that includes a succinct general mathematical description that is suitable for deriving selection rules. Then, starting with the nonlinear optical wave equation, we derive general coupled-amplitude equations for FWM of fields that vary spatially in intensity, phase, and polarization. The derived FWM theory applies to both free-space environments such as bulk nonlinear media and to weakly guiding cylindrically symmetric fibers (examples are shown in Fig. 1). We end by focusing on examples of these fields, particularly CV modes, but also circularly polarized OAM modes, and modes that are eigenstates of the total angular momentum (TAM) along z, the beam or fiber axis. For these examples, we derive and present selection rules. These spatial mode solutions are highly relevant in the development of photonic devices, since CV modes are eigenmodes of all weakly guiding cylindrically symmetric waveguides, such as standard optical fibers [16,17]. Furthermore, CV modes represent approximate solutions to the paraxial vector wave equation and, in free space, follow the intensity distribution of Laguerre–Gauss modes [18].

We begin by defining a general type of mode, those with cylindrically symmetric intensity distributions:

$$\mathbf{M}^{[u]}(r, \phi) = R^{[m]}(r)\mathbf{\Phi}^{[n]}(\phi), \tag{1}$$

where r and ϕ are the standard radial and azimuthal cylindrical coordinates, respectively, and the position is denoted as $\mathbf{r} = (r, \phi, z)$. Throughout, quantities in bold font are vectors. Here, $\mathbf{\Phi}^{[n]}(\phi)$ gives the azimuthal dependence of the polarization (which is strictly transverse) and phase for mode n. The radial dependence $R^{[m]}(r)$ is usually implicitly dependent on n
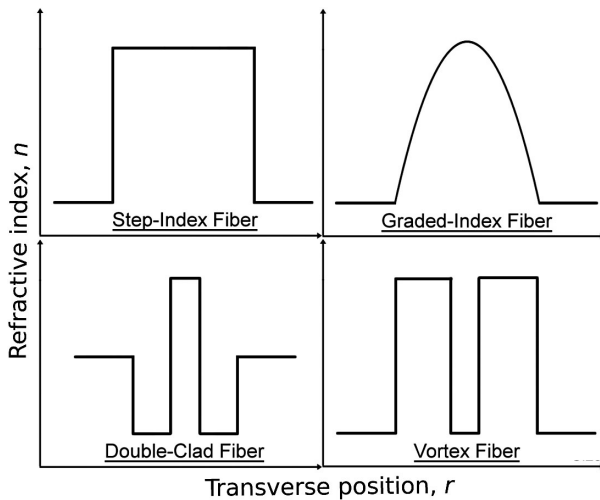

Fig. 1. Four examples (step-index, graded-index, double-clad, and vortex) of fiber types that support CV modes that are directly applicable to this work.

and will typically exhibit a number of rings in the intensity profile that equal the radial mode index m. We take u to be the set of mode indices, i.e., $u = m, n$. By defining $\mathbf{M}^{[u]}(r, \phi)$ in this way the intensity distribution is explicitly cylindrically symmetric.

Inside a cylindrically symmetric waveguide with weak guiding (e.g., with small refractive index contrast), azimuthally symmetric modes are approximate paraxial solutions to the wave equation [18]:

$$\nabla^2 \mathbf{L}(\mathbf{r}, t) + \frac{n(r)^2}{c^2}\frac{\partial^2 \mathbf{L}(\mathbf{r}, t)}{\partial t^2} \approx 0, \tag{2}$$

where $n(r)$ is the cylindrically symmetric index profile. Here, we have defined the normalized electric field solutions as

$$\mathbf{L}^{[u]}(\mathbf{r}, t) = \mathbf{M}^{[u]}(r, \phi)\exp(i\beta^{[u]}z)\exp(-i\omega t). \tag{3}$$

Each mode $\mathbf{M}^{[u]}$ has a potentially distinct effective wavevector $\beta^{[u]}$. Moreover, both the mode's radial dependence $R^{[m]}$ and $\beta^{[u]}$ depend on the angular frequency of the field ω. In contrast, given the cylindrical symmetry, $\mathbf{\Phi}^{[n]}(\phi)$ will be independent of frequency. Figure 1 shows a sample of common fiber structures to which this work is applicable.

The $\mathbf{M}^{[u]}(r, \phi)$ modes obey the following orthonormality relations [16] for transversely polarized modes:

$$\delta_{u,u'} = \int \mathbf{M}^{[u]*}(r, \phi) \cdot \mathbf{M}^{[u']}(r, \phi)r\,dr\,d\phi, \tag{4}$$

$$\delta_{m,m'} = \int R^{[m]}(r)R^{[m']}(r)r\,dr, \tag{5}$$

$$\delta_{n,n'} = \int \mathbf{\Phi}^{[n]*}(\phi) \cdot \mathbf{\Phi}^{[n']}(\phi)(r, \phi)d\phi, \tag{6}$$

where $\delta_{j,k}$ is the Kronecker delta. Here, the integral in Eq. (4) is over the transverse plane, and u and u' are composite indices incorporating all the indices of the modes. Eqs. (5) and (6) follow from Eqs. (4) and (1). Since $R^{[m]}$ depends on frequency, Eqs. (4) and (5) are strictly true only for fields of equal wavelength. This paper focuses on the azimuthal mode function $\mathbf{\Phi}^{[n]}$, which describes the spatial polarization variation of the modes. Since this variation is independent of wavelength, the $\mathbf{\Phi}$ orthonormality in Eq. (6) will also be wavelength independent. In any case, later derivations rely only on the orthonormality of modes at the same wavelength. In the next three subsections, we will introduce three types of $\mathbf{\Phi}$ modes, each of which composes a complete mode basis. Examples of the mode types are shown in Fig. 2.

A. Definite Spin and Orbital Angular Momentum Modes

The azimuthal mode function $\mathbf{\Phi}^{[n]}(\phi)$ describes both SAM and OAM. The first type of mode has a definite value for both SAM and OAM along the system axis z (e.g., the beam or fiber axis). The SAM of a photon is given by its circular polarization,

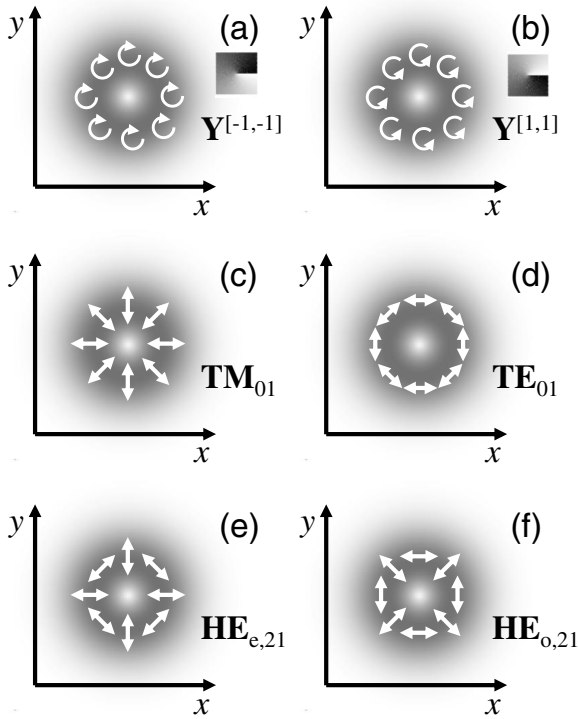$$\sigma^{[s]} = \frac{(\mathbf{x} + i\mathbf{y})}{\sqrt{2}}, \tag{7}$$

Fig. 2. Structured light modes. The gray-scale gives the intensity, arrows indicate polarization, and phase is given by the gray-scale inset. All the depicted modes have the same orbital angular magnitude, $|l| = |L| = 1$. The top two plots are spin and orbital angular momentum eigenstate modes **Y** with (a) $s = 1$ and $l = 1$ and (b) $s = -1$ and $l = -1$. The bottom four plots are cylindrical vector modes: (c) radial mode ($L = -1$, $S = 1$, TM_{01}); (d) azimuthal mode ($L = 1$, $S = -1$, TE_{01}); and hybrid modes, (e) even ($L = 1$, $S = 1$, $\mathrm{HE}_{e,21}$) and (f) odd ($L = -1$, $S = -1$, $\mathrm{HE}_{o,21}$).

with right or left circular modes yielding a spin projection along the system axis of $s\hbar$ ($s = \pm 1$). The OAM results from an azimuthal phase gradient of the field about the beam axis, $\exp(il\phi)$, and has a value of $l\hbar$ ($l = 0, \pm 1, \pm 2, \ldots$) projected along that same axis [19]. With these functions, we can define azimuthal modes $\mathbf{\Phi}^{[n]}(\phi)$ with definite values of SAM and OAM, the **Y** modes:

$$\mathbf{Y}^{[l,s]} = e^{il\phi}\boldsymbol{\sigma}^{[s]}. \qquad (8)$$

In free space, these are paraxial vector solutions to the wave equation. In waveguides, these azimuthal modes are solutions only when $l \geq 2$ [16].

B. Cylindrical Vector Modes

Our second type of $\mathbf{\Phi}$ mode is the CV mode. These are the general set of solutions in cylindrically symmetric weakly guiding waveguides, valid for $l \geq 1$ (unlike the **Y** modes). The CV azimuthal modes are

$$\mathbf{CV}^{[L,S]} = \frac{1}{\sqrt{2}}\left(e^{i\frac{\pi}{4}(S-1)}\mathbf{Y}^{[L,S]} + e^{-i\frac{\pi}{4}(S-1)}\mathbf{Y}^{[-L,-S]}\right), \quad (9)$$

where $S = \pm 1$ and $L = \pm|l|$ are mode indices. A unique feature of these modes is that in contrast to the azimuthal modes $\mathbf{Y}^{[l,s]}$,

they are real at all transverse points. The CV modes cannot be factored into functions for OAM and SAM; hence, they are non-separable and are no longer eigenstates of OAM or spin (unlike the **Y** modes). Thus, for clarity, we will henceforth refrain from referring to the spin of a particular CV mode. However, the magnitude of L does correspond to the magnitude of angular momentum l in each CV mode, $|L| = |l|$.

The CV modes can be divided into groups of four that have effective wavevector $\beta^{[u]}$ values that are close to each other [16]. Each mode in a particular mode group has an identical radial mode function (i.e., index m) and identical OAM magnitude $|l|$:

$$\mathbf{CV}^{[L=-|l|,S=1]}(\phi) = \frac{1}{\sqrt{2}}(\mathbf{Y}^{[-|l|,1]} + \mathbf{Y}^{[|l|,-1]});$$

$$(|l| = 1 : \mathrm{TM}_{0m}, |l| \geq 2 : \mathrm{EH}_{e,|l|-1,m}), \quad (10)$$

$$\mathbf{CV}^{[L=|l|,S=-1]}(\phi) = \frac{i}{\sqrt{2}}(\mathbf{Y}^{[-|l|,1]} - \mathbf{Y}^{[|l|,-1]});$$

$$(|l| = 1 : \mathrm{TE}_{0m}, |l| \geq 2 : \mathrm{EH}_{o,|l|-1,m}), \quad (11)$$

$$\mathbf{CV}^{[L=|l|,S=1]}(\phi) = \frac{1}{\sqrt{2}}(\mathbf{Y}^{[-|l|,-1]} + \mathbf{Y}^{[|l|,1]});$$

$$(|l| \geq 1 : \mathrm{HE}_{e,|l|+1,m}), \quad (12)$$

$$\mathbf{CV}^{[L=-|l|,S=-1]}(\phi) = \frac{-i}{\sqrt{2}}(\mathbf{Y}^{[-|l|,-1]} - \mathbf{Y}^{[|l|,1]});$$

$$(|l| \geq 1 : \mathrm{HE}_{o,|l|+1,m}). \quad (13)$$

The four modes above have identical intensity distributions but different patterns of spatially varying polarization. The set of modes for $|L| = 1$ is shown in Fig. 2. This ladder of modes is the mode solution to cylindrically symmetric weakly guiding waveguides.

To understand the relationship of the CV modes to the Y modes as waveguide solutions, one must consider the degeneracy of the CV modes. Some of the CV modes within each group of four will be degenerate. That is, they will have equal $\beta^{[u]}$ within the weakly guiding approximation in a waveguide. Notice that two of the four modes have OAM and SAM aligned in each term, whereas the other two modes have anti-aligned angular momenta. The aligned pair of modes in any weakly guiding cylindrically symmetric fibers are degenerate, and likewise for the anti-aligned pair. Any superposition of two degenerate modes is also a solution and has the same $\beta^{[u]}$ as the original modes. Each **Y** mode is a superposition of two degenerate CV modes and, consequently, is a waveguide-mode solution. An exception is the case of $l = \pm 1$ where the anti-aligned degeneracy is broken [16,20]. i.e., $\mathbf{CV}^{[L=-1,S=1]}$ and $\mathbf{CV}^{[L=1,S=-1]}$ are not degenerate. In summary, whereas Y modes are solutions to cylindrically symmetric weakly guiding waveguides for $l \geq 2$, CV modes are solutions for $l \geq 1$.

C. Total Angular Momentum Modes

In addition to the **CV** and **Y** mode bases, it will be useful to define a $\mathbf{\Phi}$ mode basis for the TAM projected along the beam

Table 1. Total Angular Momentum Modes

$l + s = j$	Mode
$-1 + 1 = 0$	$\mathbf{Z}^{[+0]} = \mathbf{CV}^{[L=-1, S=1]}$
$1 - 1 = 0$	$\mathbf{Z}^{[-0]} = \mathbf{CV}^{[L=1, S=-1]}$
$1 + 1 = 2$	$\mathbf{Z}^{[2]} = \mathbf{Y}^{[1,1]}$
$-1 - 1 = -2$	$\mathbf{Z}^{[-2]} = \mathbf{Y}^{[-1,-1]}$

or fiber axis. In this basis, each mode has a definite TAM of $j = l + s$, which will allow the TAM conservation to be tracked in the FWM processes. Since the FWM process occurs along the full length of the medium, this is useful to do only if these j eigenstates are also eigenmodes of the fiber, so that j is conserved during propagation. (Note: an eigenstate has a definite value of some observable, whereas an eigenmode remains unchanged upon propagation.) That is, since both FWM and linear propagation occur concurrently, it could be the linear propagation rather than the FWM that causes j to change, obscuring the role of the FWM.

For $|l| \geq 2$, these definite TAM modes will be Y modes. Since the Y modes have definite s and l, the TAM j will be definite as well. However, as explained above, for the $|l| = 1$ subspace, only two of the four Y modes are waveguide mode solutions, $\mathbf{Y}^{[1,1]}$ and $\mathbf{Y}^{[-1,-1]}$. For the other two Y modes, s and l will not be preserved during propagation. In their place, we use the anti-aligned pair of $|l| = 1$ CV modes. Notice that both superposition terms in each of these CV modes, Eqs. (10) and (11), have the same value for TAM, $l + s = j = 0$. Consequently, the anti-aligned CV modes are definite TAM states with $j = 0$. The TAM mode basis comprises these four modes, which are listed in Table 1 and are represented by Z in subsequent theory.

3. FOUR-WAVE MIXING THEORY FOR SPATIAL LIGHT MODES

We begin our FWM theory with the wave equation for a third-order nonlinear process. Unlike most other published theory, we retain the transverse vector and spatial variation of the fields. As we shall discuss later, we assume an isotropic material (such as silica) and that the nonlinearity is frequency independent. This allows us to use a simplified form for the third-order nonlinear polarization. In these systems (e.g., optical fiber), the coupled amplitude equations for the four fields are dependent on the vector eigenmodes. In our theory, the effects of self-phase modulation (SPM) and cross-phase modulation (XPM) arising from the pump beams are also included. However, SPM and XPM arising from the signal and idler are neglected on the basis that they are far less intense than the pumps. Similarly, pump depletion is also neglected in our treatment.

A. Definition of Fields

FWM converts light from two pump (p, p') fields to two outgoing fields, typically called signal (s) and idler (i), i.e., $p + p' \rightarrow s + i$. In the nondegenerate case, all four fields can have distinct frequencies and spatial modes. We define the total electric field vector in the system as the sum of the four fields:

$$\mathbf{E}(\mathbf{r}, t) = \sum_{v = p, p', s, i} \mathbf{E}_v(\mathbf{r}, t). \tag{14}$$

Each field is identified by the subscript v and is assumed to be monochromatic and exist in just one of the spatial modes discussed in Section 2. Thus, this subscript will be taken to implicitly represent the field identity (p, p', i, or s), the field frequency ω_v, and the spatial mode $\mathbf{M}^{[u]}$. When considering an individual field $\mathbf{E}_v$, we can factor out the slowly varying field amplitude $A_v(z)$:

$$\mathbf{E}_v(\mathbf{r}, t) = A_v(z)\mathbf{L}^{[u]}(\mathbf{r}, t) + \text{c.c.} \tag{15}$$

This definition will allow us to later isolate the slow change in field amplitude $A_v(z)$ due to the nonlinear interaction.

B. Nonlinear Wave Equation

The wave equation with a nonlinear source term $\mathbf{P}_{\text{NL}}$ is

$$\nabla^2 \mathbf{E}(\mathbf{r}, t) + \frac{n(r)^2}{c^2}\frac{\partial^2 \mathbf{E}(\mathbf{r}, t)}{\partial t^2} = -\mu_0 \frac{\partial^2 \mathbf{P}_{\text{NL}}(\mathbf{r}, t)}{\partial t^2}, \tag{16}$$

where μ_o is the permeability of free space, and c is the speed of light in vacuum. When considering all four fields pertinent to FWM, the left-hand side (LHS) of Eq. (16) is

$$\text{LHS[Eq. (16)]} = \sum_{v = p, p', s, i} \left[\nabla^2 \mathbf{E}_v(\mathbf{r}, t) + \frac{n(r)^2}{c^2}\frac{\partial^2 \mathbf{E}_v(\mathbf{r}, t)}{\partial t^2} \right]. \tag{17}$$

Carrying out the spatial differentiation in the Laplacian, Eq. (16) becomes

$$\text{LHS[Eq. (16)]} = \sum_{v = p, p', s, i} \left[\left(\frac{\partial^2 A_v(z)}{\partial z^2} + 2i\beta_v \frac{\partial A_v(z)}{\partial z} \right) \right.$$
$$\left. \times \mathbf{L}_v(\mathbf{r}, t) + A_v(z)\left(\nabla^2 \mathbf{L}_v(\mathbf{r}, t) + \frac{n(r)^2}{c^2}\frac{\partial^2 \mathbf{L}_v(\mathbf{r}, t)}{\partial t^2} \right) + \text{c.c.} \right]. \tag{18}$$

In the right-hand side (RHS) of the first line of this equation, we make use of the fact that $A(z)$ is assumed to be slowly varying compared to the fast oscillation associated with the effective wavevector $\beta^{[u]}$ along z. This is the slowly varying amplitude approximation, $\partial^2 A(z)/\partial z^2 = 0$. The second line is just the source-free wave equation, Eq. (2), which is zero for the solution $\mathbf{L}_v(\mathbf{r}, t)$. With these simplifications, Eq. (16) becomes

$$\sum_{v = p, p', s, i} \left[2i\beta_v \frac{\partial A_v(z)}{\partial z}\mathbf{L}_v(\mathbf{r}, t) + \text{c.c.} \right] = -\mu_0 \frac{\partial^2 \mathbf{P}_{\text{NL}}(\mathbf{r}, t)}{\partial t^2}. \tag{19}$$

C. Nonlinear Polarization and the Coupled Amplitude Equations

We now determine the form of the nonlinear polarization $\mathbf{P}_{\text{NL}}(\mathbf{r}, t)$. We omit contributions from other third-order processes such as third-harmonic generation, etc. By considering only the nonlinear polarization $\mathbf{P}_v(\mathbf{r})$ created at the pump, signal, and idler frequencies, the nonlinear polarization can be expressed as the sum

$$\mathbf{P}_{\mathrm{NL}}(\mathbf{r}, t) = \sum_{v=p, p', s, i} \mathbf{P}_v(\mathbf{r}) \exp(-i\omega_v t) + \text{c.c.} \quad (20)$$

With this definition, the RHS of the nonlinear wave equation, Eq. (19), becomes

$$\text{RHS[Eq. (19)]} = \mu_0 \sum_{v=p, p', s, i} \omega_v^2 \mathbf{P}_v(\mathbf{r}) \exp(-i\omega_v t) + \text{c.c.} \quad (21)$$

In materials that are both isotropic and satisfy the Kleinman symmetry condition (i.e., the frequency dependence of $\chi^{(3)}$ can be neglected [21]), the third-order nonlinear susceptibility tensor can be expressed in terms of a single scalar component (i.e., $\chi_{xxxx}^{(3)}$). As we show in Appendix A, the nonlinear polarization at the signal frequency is then given by

$$\mathbf{P}_s(\mathbf{r}) = 2\epsilon_0 \chi_{xxxx}^{(3)} [(\mathbf{E}_p^* \cdot \mathbf{E}_p) \mathbf{E}_s + (\mathbf{E}_p^* \cdot \mathbf{E}_s) \mathbf{E}_p + (\mathbf{E}_p \cdot \mathbf{E}_s) \mathbf{E}_p^*$$
$$+ (\mathbf{E}_{p'}^* \cdot \mathbf{E}_{p'}) \mathbf{E}_s + (\mathbf{E}_{p'}^* \cdot \mathbf{E}_s) \mathbf{E}_{p'} + (\mathbf{E}_{p'} \cdot \mathbf{E}_s) \mathbf{E}_{p'}^*$$
$$+ (\mathbf{E}_i^* \cdot \mathbf{E}_p) \mathbf{E}_{p'} + (\mathbf{E}_i^* \cdot \mathbf{E}_{p'}) \mathbf{E}_p + (\mathbf{E}_p \cdot \mathbf{E}_{p'}) \mathbf{E}_i^*], \quad (22)$$

where we have omitted the spatial–temporal coordinates for clarity. A similar equation can be found for the nonlinear polarization at the idler frequency $\mathbf{P}_i$ by exchanging s and i throughout Eq. (22). The first six terms in Eq. (22) represent XPM from the pump beams, and the last three terms are the contribution to FWM.

Now that we have a succinct form for the nonlinear polarization, we can evaluate its action on the signal and idler fields. The nonlinear wave equation [Eq. (19)] for just the signal field is

$$2i\beta_s \frac{\partial A_s(z)}{\partial z} \mathbf{M}_s(r, \phi) \exp(i\beta_s z) = \frac{\omega_s^2 \mathbf{P}_s(\mathbf{r})}{\epsilon_0 c^2}. \quad (23)$$

Substituting in the nonlinear polarization of the signal frequency $\mathbf{P}_s$ from Eq. (22) into Eq. (23), we obtain

$$\frac{\partial A_s(z)}{\partial z} \mathbf{M}_s = \frac{-i\omega_s^2 \chi_{xxxx}^{(3)}}{2\beta_s c^2} \{ A_p^* A_p A_s [\boldsymbol{\alpha}_{pps} + \boldsymbol{\alpha}_{psp} + \bar{\boldsymbol{\alpha}}_{psp}]$$
$$+ A_{p'}^* A_{p'} A_s [\boldsymbol{\alpha}_{p'p's} + \boldsymbol{\alpha}_{p'sp'} + \bar{\boldsymbol{\alpha}}_{p'sp'}]$$
$$+ A_p A_{p'} A_i^* [\boldsymbol{\alpha}_{ipp'} + \boldsymbol{\alpha}_{ip'p} + \bar{\boldsymbol{\alpha}}_{pp'i}] \exp(i\Delta kz) \}, \quad (24)$$

where $\Delta k = \beta_p + \beta_{p'} - \beta_s - \beta_i$ is the phasematching term and where we introduce the quantities $\boldsymbol{\alpha}_{ijk} = (\mathbf{M}_i^* \cdot \mathbf{M}_j)\mathbf{M}_k$ and $\bar{\boldsymbol{\alpha}}_{ijk} = (\mathbf{M}_i \cdot \mathbf{M}_j)\mathbf{M}_k^*$. As before, we have suppressed the dependence of A and $\mathbf{M}$ on the spatial coordinates.

We now isolate the behavior of the scalar amplitudes A by taking the dot product with $\mathbf{M}_s^*$ on both sides and integrating over the transverse plane. With this, the orthonormality condition in Eq. (4) yields the coupled amplitude equation for the signal (or idler, by exchanging s and i throughout) as

$$\frac{\partial A_s(z)}{\partial z} = \kappa_s \{ |A_p|^2 A_s [\mathsf{O}_{p^*ps^*s} + \mathsf{O}_{p^*ss^*p} + \mathsf{O}_{pss^*p^*}]$$
$$+ |A_{p'}|^2 A_s [\mathsf{O}_{p'^*p's^*s} + \mathsf{O}_{p'^*ss^*p'} + \mathsf{O}_{p'ss^*p'^*}]$$
$$+ A_p A_{p'} A_i^* [\mathsf{O}_{i^*ps^*p'} + \mathsf{O}_{i^*p's^*p} + \mathsf{O}_{pp's^*i^*}]$$
$$\times \exp(i\Delta kz) \}. \quad (25)$$

Here, the field coupling constant κ_s is given by $\kappa_s = \frac{-i\omega_s^2 \chi_{xxxx}^{(3)}}{2\beta_s c^2}$, and $\mathsf{O}_{a^{(*)}b^{(*)}c^{(*)}d^{(*)}} = \int (\mathbf{M}_a^{(*)} \cdot \mathbf{M}_b^{(*)})(\mathbf{M}_c^{(*)} \cdot \mathbf{M}_d^{(*)}) r \, dr \, d\phi$ is the mode overlap integral. In $\mathsf{O}_{a^{(*)}b^{(*)}c^{(*)}d^{(*)}}$, the subscripts a, b, c, and d represent the fields (p, p', s, or i) and an optional conjugate on a particular subscript applies to the corresponding mode in the integral. For example, $\mathsf{O}_{i^*ps^*p'} = \int (\mathbf{M}_i^* \cdot \mathbf{M}_p)(\mathbf{M}_s^* \cdot \mathbf{M}_{p'}) r \, dr \, d\phi$. So far, we have not used the cylindrical symmetry of the modes. This coupled wave equation is applicable in bulk media and waveguides since it only assumes that $\mathbf{M}_v$ are paraxial modes that are approximate solutions to the wave equation. (In Appendix A, we give the analogous coupled amplitude equation for the pump field.)

We now consider the conditions necessary for efficient FWM. The first two lines on the RHS of Eq. (25) describe XPM in the signal field induced by the pumps. The last line describes FWM. FWM requires perfect energy conservation and is most efficient when photon momentum is also conserved. These two conditions constitute perfect phasematching, $\Delta\omega = \omega_p + \omega_{p'} - \omega_i - \omega_s = 0$ and $\Delta k = 0$, which can occur in many different FWM processes since β_v varies with mode and frequency [21]. For example, different CV-mode combinations in the FWM process will be phasematched at different sets of frequencies. Since the energy and momentum conservation for FWM will depend on the specific medium and waveguide of interest, we will not further consider the details of phasematching in this paper.

The selection rules arise from a third condition for FWM. Namely, in the final line of the coupled wave equation, Eq. (25), the total process amplitude,

$$\mathsf{U} \equiv \mathsf{O}_{i^*ps^*p'} + \mathsf{O}_{i^*p's^*p} + \mathsf{O}_{pp's^*i^*}, \quad (26)$$

must be non-zero.

4. FOUR-WAVE MIXING SELECTION RULES

So far, the coupled wave equations have been derived for any transverse modes satisfying the linear wave equation. We now restrict ourselves to systems with cylindrical symmetry, such as optical fibers. We introduce cylindrically symmetric modes into the FWM integrals listed in Eq. (26) in order to find a set of selection rules based on the transitions permitted between the modes. To start, we use the mode definition in Eq. (1) to separate the overlap integrals comprising the process amplitude U into a product of radial and azimuthal parts such that

$$\mathsf{O}_{a^{(*)}b^{(*)}c^{(*)}d^{(*)}} = F \int (\boldsymbol{\Phi}_a^{(*)} \cdot \boldsymbol{\Phi}_b^{(*)})(\boldsymbol{\Phi}_c^{(*)} \cdot \boldsymbol{\Phi}_d^{(*)}) \, d\phi, \quad (27)$$

where $F \equiv \int R_i^* R_p R_s^* R_{p'} r \, dr$ is the integral over the radial dependence. Since the radial mode function $R_v = R^{[m(v)]}(r)$ depends on the specific radial index profile $n(r)$ of a chosen waveguide, we will focus on the selection rules set by the azimuthal modes. These selection rules will then be general to any medium with cylindrical symmetry. Specifically, we assume that F is non-zero, as would be true if all four fields were in the same radial mode (i.e., the same value of m). Henceforth, a "mode" will refer only to its azimuthal component $\mathbf{\Phi}_v (\phi)$. (Note that for the CV mode basis only, the potential complex conjugates of $\mathbf{\Phi}_v$ in the integral Eq. (27) can be dismissed since at all transverse positions the modes are real.)

The total FWM intensity is proportional to the sum U, Eq. (26), of three overlap integrals, each of which is defined by Eq. (27). By considering the mode combinations for the four fields that lead to a non-zero U, we can find the corresponding sets of selection rules for a given set of mode indices. We will express allowed FWM processes in the notation, $\mathbf{M}_p + \mathbf{M}_{p'} \rightarrow \mathbf{M}_i + \mathbf{M}_s$. All allowed processes can also occur in reverse, i.e., with input and output modes interchanged. If a process occurs for a particular set of modes in fields p and p', then it will also occur with the modes interchanged between p and p' and likewise for output fields s and i.

Of particular interest is the scenario where all the involved modes are taken from the family of four modes (within the Y, CV, and Z mode types) that have equal $|l|$. With this limited set of four, there is a finite number of potential processes, which we will determine.

A. Summary of the Y Mode Selection Rules

For the sake of completeness and for use later, we derive the selection rules for fields in the Y angular momentum modes. Our results agree with similar FWM studies involving linearly polarized modes [9]. We insert combinations of Y modes into the three O overlap integrals inside U [Eq. (26)]. Each overlap integral factors into OAM and SAM components. For example,

$$\mathsf{O}_{i^* p s^* p'} = F \left(\boldsymbol{\sigma}^{[-s_i]} \cdot \boldsymbol{\sigma}^{[s_p]} \right) \left(\boldsymbol{\sigma}^{[-s_s]} \cdot \boldsymbol{\sigma}^{[s_{p'}]} \right)$$

$$\times \int e^{i \left(-l_i + l_p - l_s + l_{p'} \right) \phi} \, d\phi$$

$$= F \delta_{s_i, s_p} \delta_{s_s, s_{p'}} \delta_{l_p + l_{p'}, l_s + l_i}. \tag{28}$$

The other two O integrals give similar results. Given that s is limited to the values ± 1, the Kronecker deltas for the s values in the three integrals can be combined to arrive at the selection rules

$$s_p + s_{p'} = s_i + s_s,$$

$$l_p + l_{p'} = l_i + l_s, \tag{29}$$

where l_v and s_v are the mode indices of fields $v = p, p', s, i$. When these rules are satisfied, the process will occur with amplitude $\mathsf{U} = 4\pi F$. We give a more detailed derivation of this in Appendix B.

These two rules show that SAM and OAM are independently conserved. That is, there is no coupling between the SAM and

Table 2. Selection Rules for CV Modes

Rule	L	S	Process Amplitude, U
1	$L_p + L_{p'} = L_s + L_i$	$S_p + S_{p'} = S_s + S_i$	$2\pi F$
2	$L_p + L_{p'} = -(L_s + L_i)$	$S_p + S_{p'} = -(S_s + S_i)$	$-2\pi F$
3	$L_p - L_{p'} = L_s - L_i$	$S_p - S_{p'} = S_s - S_i$	$2\pi F$
4	$L_p - L_{p'} = -(L_s - L_i)$	$S_p - S_{p'} = -(S_s - S_i)$	$2\pi F$

OAM degrees of freedom. Consequently, the only way for the TAM along the fiber or beam axis, $j = l + s$, to be conserved is for SAM to be conserved and OAM to be conserved:

$$\Delta s = s_p + s_{p'} - s_s - s_i = 0,$$

$$\Delta l = l_p + l_{p'} - l_s - l_i = 0,$$

$$\Delta j = j_p + j_{p'} - j_s - j_i = 0. \tag{30}$$

In other words, in the weakly guiding or paraxial approximation, TAM cannot be conserved by converting SAM into OAM. This is a result of the fact that in these approximations, the fields are transverse everywhere.

B. Summary of the CV Mode Selection Rules

We now consider the situation in which each of the four fields is in a CV mode. Each mode can have any value of $|L|$. We label the mode indices for field $v = p, p', s, i$ as L_v and S_v. Table 2 gives the four selection rules from our derivation, which is detailed in Appendix B. More than one rule can hold true simultaneously, and their amplitudes should be added to find the total process amplitude U. Since S is limited to ± 1, the selection rules disallow processes where there is an odd number of like S values among i, s, p, and p'.

We now consider the limited situation in which all the modes have the same value of $|L|$. As an example of this, we will identify the relevant modes for $|L| = 1$ (i.e., TM, TE, etc.), but the results hold for all $|L|$. We compile all 100 distinct possible processes in a table in Fig. 3 (see Appendix B for a discussion of counting distinct processes). Now, similar to the situation for S, since L is limited to $\pm |L|$, the selection rules disallow processes where there is an odd number of like L values among i, s, p, and p'. This is confirmed by the table, which shows that processes where any given mode (e.g., TE) does not appear in pairs is ruled out. For example, TM + TE → TM + TE or $HE_e + HE_e \rightarrow HE_e + HE_e$ or TM + TM → $HE_o + HE_o$ is allowed but TM + TE → TM + TM is not. This single selection rule is similar to the selection rules for linear polarized fields in an isotropic medium [10] that involve only two orthogonal polarizations. Examples of possible CV mode conversions for total amplitudes ranging from $2\pi F$ to $6\pi F$ are shown in Fig. 4.

When considering higher-order CV modes beyond the $|L| = 1$ manifold, one can find non-trivial allowed FWM processes such as $L_p = 2$, $L_{p'} = 2$, $L_s = 3$, and $L_i = 1$ among others. However, since radial functions $R^{[m]}(r)$ typically implicitly depend on $|l|$, they will have different shapes for each mode. In turn, this will decrease the radial overlap integral F and, thus, these processes will occur with decreased efficiency.

The matrix of process amplitudes U (Fig. 3). Output modes (S_1, L_1, S_2, L_2) across top; input modes down the left.

				S_1	L_1	S_2	L_2
				1	1	1	1
				1	1	1	-1
				1	1	-1	1
				1	-1	1	-1

Output rows (HEe HEe / HEe TM / ... columns):

Input \ Output pair	HEe HEe	HEe TM	HEe TE	HEe HEo	TM TM	TE TE	TE TM	HEo TM	HEo TE	HEo HEo
S_1	1	1	1	1	1	-1	-1	-1	-1	-1
L_1	1	1	1	1	-1	1	1	-1	-1	-1
S_2	1	1	-1	-1	1	-1	1	1	-1	-1
L_2	1	-1	1	-1	-1	1	-1	-1	1	-1

Input ($S_1 L_1 S_2 L_2$)					HEe HEe	HEe TM	HEe TE	HEe HEo	TM TM	TE TE	TE TM	HEo TM	HEo TE	HEo HEo
HEe HEe	1	1	1	1	3	0	0	0	2	2	0	0	0	1
HEe TM	1	1	1	-1	0	2	0	0	0	0	0	0	0	0
HEe TE	1	1	-1	1	0	0	2	0	0	0	0	0	0	0
HEe HEo	1	1	-1	-1	0	0	0	1	0	0	0	0	0	0
TM TM	1	-1	1	-1	2	0	0	0	3	1	0	0	0	2
TE TE	-1	1	-1	1	2	0	0	0	1	3	0	0	0	2
TE TM	-1	1	1	-1	0	0	0	0	0	0	1	0	0	0
HEo TM	-1	-1	1	-1	0	0	0	0	0	0	0	2	0	0
HEo TE	-1	-1	-1	1	0	0	0	0	0	0	0	0	2	0
HEo HEo	-1	-1	-1	-1	1	0	0	0	2	2	0	0	0	3

Allowed processes — input ($S_1\ L_1\ S_2\ L_2$)

Fig. 3. Process amplitudes U for four-wave mixing between CV modes. All four modes have the same value of $|L| = |l|$. Here, we take $|l| = 1$, but the amplitudes for $|l| > 1$ are identical to these. The process amplitudes in the table are calculated from Eq. (B16) and are normalized as $\mathsf{U}/2\pi F$.
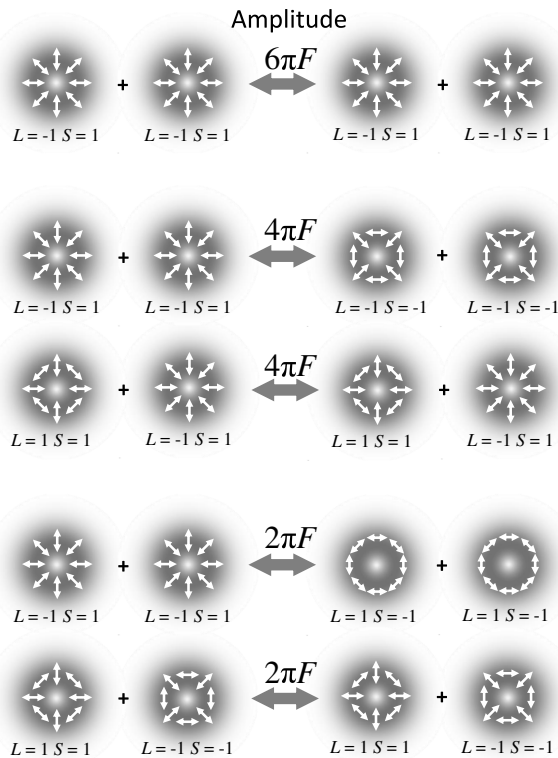

Fig. 4. Examples of allowed four-wave mixing processes between cylindrical vector modes.

C. Selection Rules for the TAM Mode Basis

We now consider the situation in which each of the four fields is in a TAM mode. The TAM mode set consists of the two $j = 0$ modes, $\mathbf{Z}^{[-0]} = \mathbf{CV}^{[-1,1]}$ and $\mathbf{Z}^{[+0]} = \mathbf{CV}^{[1,-1]}$, and the $j = \pm 2$ modes $\mathbf{Y}^{[1,1]}$ and $\mathbf{Y}^{[-1,-1]}$. A derivation of the relevant selection rules is given in Appendix B. Here, we summarize them and consider if conservation of TAM is enforced by the rules. In particular, we ask whether the sum of the TAM of the two input photons is conserved in FWM, $j_i + j_s = j_p + j_{p'}$.

Of the 100 potential processes, the ones involving solely Y modes or solely Z modes are already treated by the selection rules in the last two sections. We have already shown that the selection rules for the Y modes conserve j since they separately conserve OAM and SAM. However, the Z modes are not eigenstates of OAM or SAM, and, thus, one cannot ascribe s and l values before and after the process. It follows that it becomes impossible to evaluate their conservation. Instead, we directly consider the TAM, j. A process containing only Z modes trivially conserves the two photons' TAM, given that each mode carries none. Thus, we focus on the non-trivial processes that interconvert $j = 0$ and $j = \pm 2$ modes, which we summarize in Table 3.

Considering the conservation of angular momentum, the first allowed process reads $j_i + j_s - j_p - j_{p'} = \mp 2 \pm 2 - 0 - 0 = 0$. The second process, the reverse of the first, conserves TAM in a similar manner. The last process reads $j_i + j_s - j_p - j_{p'} = 0 \pm 2 - 0 \mp 2 = 0$. Thus, all the TAM interconversion processes conserve TAM of the two photons.

One might ask whether conservation of TAM could be used as the sole selection rule. The answer is no. There are many processes that would conserve TAM that are not permitted, such as $\mathbf{Z}^{[+0]} + \mathbf{Y}^{[\pm 1, \pm 1]} \to \mathbf{Z}^{[-0]} + \mathbf{Y}^{[\pm 1, \pm 1]}$. Allowed processes can occur with different amplitudes of $\mathsf{U} = 2\pi F$, $4\pi F$, and $6\pi F$.

D. Prospects for the Generation of Mode-Entangled Photon Pairs

In spontaneous FWM, vacuum-state fields in any chosen pair of input signal and idler modes (since all the possible input modes contain vacuum) undergo FWM with a strong pump field. The mixing will occasionally produce a pair of photons, one in the output idler field and one in the output signal field. This will occur with the same relative amplitude as the corresponding FWM process. Consequently, for any given two input pump modes, the FWM selection rules identify signal and idler output

Table 3.   Selection Rules for Definite Total Angular Momentum Modes

Process Type	Allowed Processes	Amplitude, $\mathsf{U}^{(TAM)}$
$\mathbf{Z}^{[w0]} + \mathbf{Z}^{[w0]} \to \mathbf{Y}^{[q,q]} + \mathbf{Y}^{[-q,-q]}$	$w = \pm,$ $q = \pm 1$	$4\pi F$
$\mathbf{Y}^{[q,q]} + \mathbf{Y}^{[-q,-q]} \to \mathbf{Z}^{[w0]} + \mathbf{Z}^{[w0]}$	$w = \pm,$ $q = \pm 1$	$4\pi F$
$\mathbf{Z}^{[w0]} + \mathbf{Y}^{[q,q]} \to \mathbf{Z}^{[w0]} + \mathbf{Y}^{[q,q]}$	$w = \pm,$ $q = \pm 1$	$4\pi F$

mode combinations that SFWM will produce photon pairs in. That is, it identifies allowed SFWM processes.

Previous work has generated photon pairs that are entangled in their OAM modes [22]. In those cases, entanglement occurred naturally through the conservation of OAM. More generally, to generate entanglement through a spontaneous nonlinear process such as downconversion or FWM, one requires two simultaneous processes that each produce a different pair of signal and idler modes. In order to generate entanglement, the modes containing the signal and idler photons must be indistinguishable other than in the degree of freedom that is entangled [23]. For FWM in a fiber, this entails phasematching the two processes with identical signal wavelengths and identical idler wavelengths. Since each mode has a different effective wavevector β with different dependences on wavelength, Δk will typically vary differently with wavelength for the two processes. Consequently, such phasematching is nontrivial. Fortunately, control of the effective index β can be achieved by careful design of the fiber index profile and choice of material [24].

In order for these two processes together to create mode entanglement, they must produce different pairs of modes, $\mathbf{M}_i$ and $\mathbf{M}_s$, from one another. An example of two appropriate processes is $\mathbf{Y}_p^{[1,1]} + \mathbf{Y}_{p'}^{[-1,-1]} \rightarrow \mathbf{Z}_i^{[+0]} + \mathbf{Z}_s^{[+0]}$ and $\mathbf{Y}_p^{[1,1]} + \mathbf{Y}_{p'}^{[-1,-1]} \rightarrow \mathbf{Z}_i^{[-0]} + \mathbf{Z}_s^{[-0]}$. The entangled state of the two spontaneously generated photons would be $\mathbf{Z}_i^{[+0]}\mathbf{Z}_s^{[+0]} + \mathbf{Z}_i^{[-0]}\mathbf{Z}_s^{[-0]}$. The availability of many allowed FWM processes for cylindrical vector modes means that there are many possibilities for the generation of photons entangled in their spatial-polarization modes.

5. CONCLUSION

In conclusion, we present a theoretical investigation into the nonlinear optics of structured light. Specifically, we developed a theory describing FWM of CV modes in optical fiber or free space and the mode selection rules that follow. For comparison, we also review analogous theory for modes with definite SAM and OAM. Given the cylindrical symmetry of a fiber and free space, one might expect that the only quantity that must be strictly conserved in FWM is the TAM along the system axis. Indeed, in some processes, OAM and SAM are independently conserved and, thus, so too will be the TAM. However, for OAM $|l| = 1$, the fundamental eigenmodes of an optical fiber are not eigenstates of either SAM or OAM, and, consequently, these properties will change during propagation. Nonetheless, we showed that for modes that are TAM eigenstates, the sum of two photons' TAM is conserved and emerges in the output photons. Future work will investigate the link between FWM selection rules and angular momentum conservation laws outside of the paraxial and weakly guiding regime.

Since CV modes are the eigenmodes of weakly guiding fibers and of free-space propagation, the selection rules presented here are pertinent to a range of applications. These include telecommunications, where structured modes can increase bandwidths [1,2]. Additionally, our results could find use in all-optical switching by utilizing the optical nonlinearity of structured spatial modes as a way to route such beams. In quantum optics, CV modes are currently being investigated for use in quantum cryptography [25]. Using our results, the CV mode photons could be generated directly by FWM inside optical fibers. We also show how to generate photon pairs entangled in their CV modes. Beyond fiber optics, our results have implications in free-space FWM, and could shed light on the debate over the roles of SAM and OAM in photons [26,27].

APPENDIX A: DERIVATION OF THE FUNCTIONAL FORM OF THE NONLINEAR POLARIZATION

In this appendix, we will derive the form of the third-order nonlinear polarization $\mathbf{P}$ for an isotropic material. In general, each component P_i ($i = x, y, z$) of the $\chi^{(3)}$ nonlinear polarization for a given process is [21]

$$P_i = \epsilon_0 D \sum_{jkl=x,y,z} \chi_{ijkl}^{(3)} E_j(\omega_o) E_k(\omega_n) E_l(\omega_m), \qquad \textbf{(A1)}$$

where the degeneracy factor D is equal to the number of distinct permutations of the fields. For the moment, all subscripts refer to Cartesian coordinates x, y, z unlike in the main body of the paper, where subscripts p, p', s, and i identify the field.

The non-zero components of the $\chi^{(3)}$ tensor are

$$\chi_{xxyy}^{(3)} = \chi_{xxzz}^{(3)} = \chi_{yyxx}^{(3)} = \chi_{yyzz}^{(3)} = \chi_{zzxx}^{(3)} = \chi_{zzyy}^{(3)}$$

$$= \chi_{xyxy}^{(3)} = \chi_{xzxz}^{(3)} = \chi_{yzyz}^{(3)} = \chi_{yxyx}^{(3)} = \chi_{zxzx}^{(3)} = \chi_{zyzy}^{(3)}$$

$$= \chi_{xyyx}^{(3)} = \chi_{xzzx}^{(3)} = \chi_{yxxy}^{(3)} = \chi_{yzzy}^{(3)} = \chi_{zxxz}^{(3)} = \chi_{zyyz}^{(3)}$$

$$= \frac{1}{3}\chi_{xxxx}^{(3)} = \frac{1}{3}\chi_{yyyy}^{(3)} = \frac{1}{3}\chi_{zzzz}^{(3)}. \qquad \textbf{(A2)}$$

Since most of the $\chi^{(3)}$ tensor components are zero, for each nonlinear polarization component P_i, only seven terms of the 27-term sum are non-zero. The last line of Eq. (A2) shows that the $jkl = iii$ term is multiplied by a factor of three. Instead, we divide the iii term into three separate terms in order to make evident an upcoming vector product. All together then, there are nine non-zero terms in the nonlinear polarization:

$$P_i = \frac{\epsilon_0 D \chi_{xxxx}^{(3)}}{3}\big[(E_i(\omega_o) E_i(\omega_n) + E_j(\omega_o) E_j(\omega_n)$$

$$+ E_k(\omega_o) E_k(\omega_n)) E_i(\omega_m) + (E_i(\omega_n) E_i(\omega_m)$$

$$+ E_j(\omega_n) E_j(\omega_m) + E_k(\omega_n) E_k(\omega_m)) E_i(\omega_o)$$

$$+ (E_i(\omega_o) E_i(\omega_m) + E_j(\omega_o) E_j(\omega_m)$$

$$+ E_k(\omega_o) E_k(\omega_m)) E_i(\omega_n) \big]$$

$$= \frac{\epsilon_0 D \chi_{xxxx}}{3}\big[(\mathbf{E}(\omega_o) \cdot \mathbf{E}(\omega_n)) E_i(\omega_m) (\mathbf{E}(\omega_m)$$

$$\cdot \mathbf{E}(\omega_n)) E_i(\omega_o) (\mathbf{E}(\omega_m) \cdot \mathbf{E}(\omega_o)) E_i(\omega_n) \big], \qquad \textbf{(A3)}$$

where i, j, and k are any permutation of $\{x, y, z\}$. We have also assumed that the frequency dependence of the susceptibility can be neglected (the Kleinman symmetry condition). Writing the three polarization Cartesian components as a vector, we have

$$\mathbf{P} = \frac{\epsilon_0 D \chi^{(3)}_{xxxx}}{3}[(\mathbf{E}(\omega_o) \cdot \mathbf{E}(\omega_n))\mathbf{E}(\omega_m)$$

$$+ (\mathbf{E}(\omega_m) \cdot \mathbf{E}(\omega_n))\mathbf{E}(\omega_o) + (\mathbf{E}(\omega_m) \cdot \mathbf{E}(\omega_o))\mathbf{E}(\omega_n)]. \quad \textbf{(A4)}$$

In the main text, the nonlinear polarization in Eq. (22) follows from applying this to FWM and XPM (conjugating fields with negative frequency) and evaluating the degeneracy factor: $D = 6$ for three distinct fields and $D = 3$ for two distinct fields.

For completeness, the nonlinear polarization for the pump p (or p', by exchanging p and p' throughout) is

$$\mathbf{P}_p(\mathbf{r}) = \epsilon_0 \chi^{(3)}_{xxxx}[(\mathbf{E}_p \cdot \mathbf{E}_p)\mathbf{E}_p^* + 2(\mathbf{E}_p^* \cdot \mathbf{E}_p)\mathbf{E}_p$$

$$+ 2(\mathbf{E}_{p'}^* \cdot \mathbf{E}_{p'})\mathbf{E}_p + 2(\mathbf{E}_{p'} \cdot \mathbf{E}_p)\mathbf{E}_{p'}^* + 2(\mathbf{E}_{p'}^* \cdot \mathbf{E}_p)\mathbf{E}_{p'}]. \quad \textbf{(A5)}$$

Here, the subscripts on the electric fields and polarization indicate the field identity, p or p'. By the same procedure used in the main body of the paper, the coupled equations for the pump amplitude p (and p', by exchanging p and p' throughout) are found to be

$$\frac{\partial A_p(z)}{\partial z} = \frac{1}{2}\kappa_p \{|A_p|^2 A_p \left[\mathsf{O}_{ppp^*p^*} + 2\mathsf{O}_{p^*pp^*p}\right]$$

$$+ 2|A_{p'}|^2 A_p \left[\mathsf{O}_{p'^*p'p^*p} + \mathsf{O}_{p'pp^*p'^*} + \mathsf{O}_{p'^*pp^*p'}\right]\}. \quad \textbf{(A6)}$$

APPENDIX B: CALCULATION OF FOUR-WAVE MIXING PROCESS AMPLITUDES

In this appendix, we outline how to evaluate the overlap integral, $\mathsf{O}_{a(*)b(*)c(*)d(*)} = F \int (\boldsymbol{\Phi}_a^{(*)} \cdot \boldsymbol{\Phi}_b^{(*)})(\boldsymbol{\Phi}_c^{(*)} \cdot \boldsymbol{\Phi}_d^{(*)})\mathrm{d}\phi$. The sum of three O integrals gives the FWM process amplitude $\mathsf{U} = \mathsf{O}_{i^*ps^*p'} + \mathsf{O}_{i^*p's^*p} + \mathsf{O}_{pp's^*i^*}$ for the set of modes in fields $v = p, p', s, i$. We label the mode indices for field v with the corresponding subscript, e.g., s_p, L_i, or S_s. As explained in the main body of the paper, a complex conjugate on the field v in the subscript of O indicates the corresponding mode should be conjugated, i.e., $\boldsymbol{\Phi}_v^*$. In all three O integrals, two of the indices are conjugated.

1. Process Amplitudes for Definite Spin and Orbital Angular Momentum States

We start by considering FWM processes in which all four beams are in OAM and SAM eigenstate modes, $\mathbf{Y}^{[l,s]} = e^{il\phi}\boldsymbol{\sigma}^{[s]}$. The process amplitude $\mathsf{U}^{(Y)}$ is calculated from the coupled amplitude equation for the signal Eq. (4). The terms comprising the FWM process amplitude are formed by the product of four $\mathbf{Y}$ modes. We begin with half of this product: the dot product of two general $\mathbf{Y}$ modes. For fields a and b, this is

$$\mathbf{Y}_a^{(*)} \cdot \mathbf{Y}_b^{(*)} = \boldsymbol{\sigma}^{[\pm s_a]} \cdot \boldsymbol{\sigma}^{[\pm s_b]}e^{i(\pm l_a \pm l_b)\phi}. \quad \textbf{(B1)}$$

Here, $(*)$ indicates the optional presence of the complex conjugate on $\boldsymbol{\Phi}_v$, in which case, each mode index of the v field (e.g., s_v) is preceded by the bottom symbol of $\pm$ or $\mp$. Using $\boldsymbol{\sigma}^{[s]} = \frac{(\mathbf{x} + is\mathbf{y})}{\sqrt{2}}$ with $s = \pm 1$, it holds that $\boldsymbol{\sigma}^{[s_i]} \cdot \boldsymbol{\sigma}^{[s_j]} = \delta_{s_i, -s_j}$. The full argument of one overlap integral is then

$$\mathsf{O}_{a(*)b(*)c(*)d(*)} = F \int \left(\mathbf{Y}_a^{(*)} \cdot \mathbf{Y}_b^{(*)}\right)\left(\mathbf{Y}_c^{(*)} \cdot \mathbf{Y}_d^{(*)}\right)\mathrm{d}\phi$$

$$= \delta_{\pm s_a, \mp s_b}\delta_{\pm s_c, \mp s_d} F \int e^{i(\pm l_a \pm l_b \pm l_c \pm l_d)\phi}\mathrm{d}\phi$$

$$= 2\pi F \delta_{\pm s_a, \mp s_b}\delta_{\pm s_c, \mp s_d}\delta_{0,(\pm l_a \pm l_b \pm l_c \pm l_d)}, \quad \textbf{(B2)}$$

where in the last line, we use $\int_0^{2\pi} \exp(iq\phi)\mathrm{d}\phi = 2\pi\delta_{0,q}$. Using this result, the three O integrals composing $\mathsf{U}^{(Y)}$ are

$$\mathsf{O}_{i^*ps^*p'} = 2\pi F \delta_{s_i,s_p}\delta_{s_s,s_{p'}}\delta_{l_p+l_{p'},l_i+l_s}, \quad \textbf{(B3)}$$

$$\mathsf{O}_{i^*p's^*p} = 2\pi F \delta_{s_i,s_{p'}}\delta_{s_s,s_p}\delta_{l_p+l_{p'},l_i+l_s}, \quad \textbf{(B4)}$$

$$\mathsf{O}_{pp's^*i^*} = 2\pi F \delta_{s_p,-s_{p'}}\delta_{-s_s,s_i}\delta_{l_p+l_{p'},l_i+l_s}. \quad \textbf{(B5)}$$

The total process amplitude is then the summation of Eqs. (B2)–(B5):

$$\mathsf{U}^{(Y)} = 2\pi F \left(\delta_{s_i,s_p}\delta_{s_s,s_{p'}} + \delta_{s_i,s_{p'}}\delta_{s_s,s_p} + \delta_{s_p,-s_{p'}}\delta_{-s_s,s_i}\right)$$

$$\times \delta_{l_p+l_{p'},l_i+l_s}$$

$$= 4\pi F \delta_{s_i+s_s,s_p+s_{p'}}\delta_{l_i+l_s,l_p+l_{p'}}, \quad \textbf{(B6)}$$

where the last line uses an identity that we will introduce in the next section. Each Kronecker delta provides a selection rule: $s_i + s_s = s_p + s_{p'}$ and $l_i + l_s = l_p + l_{p'}$, or more succinctly, $\Delta s = 0$ and $\Delta l = 0$. In summary, the SAM and OAM are independently conserved in the FWM process.

2. Process Amplitudes for the CV Modes

We now calculate the process amplitude $\mathsf{U}^{(CV)}$ for a FWM process where all the beams are in CV modes. A CV mode consists of a superposition of two $\mathbf{Y}$ modes, as in Eq. (9):

$$\mathbf{CV}^{[L,S]} = \frac{1}{\sqrt{2}}\left(e^{i\frac{\pi}{4}(S-1)}\mathbf{Y}^{[L,S]} + e^{-i\frac{\pi}{4}(S-1)}\mathbf{Y}^{[-L,-S]}\right). \quad \textbf{(B7)}$$

Since these modes are real, we drop the complex conjugates in O. The mode overlap integral, Eq. (27), contains two inner products of two CV modes each. When expanded using Eq. (9), O contains 16 terms, each containing a $\mathbf{Y}$ mode factor from all four fields, $v = a, b, c, d$. From Eq. (B7), each of these four $\mathbf{Y}$ mode factors will be either of the form $\mathbf{Y}^{[+L_v,+S_v]}$ or $\mathbf{Y}^{[-L_v,-S_v]}$. Consequently, we represent these 16 terms as a sum indexed by the sign of the S and L values, as represented by $n_v = \pm 1$:

$$O_{abcd} = F \int \left(\mathbf{CV}^{[L_a, S_a]} \cdot \mathbf{CV}^{[L_b, S_b]} \right) \left(\mathbf{CV}^{[L_c, S_c]} \cdot \mathbf{CV}^{[L_d, S_d]} \right) \mathrm{d}\phi$$

$$= \frac{F}{4} \sum_{n_a..n_d = \pm 1} e^{i \frac{\pi}{4}(n_a S_a + n_b S_b + n_c S_c + n_d S_d - K)}$$

$$\times \int \left(\mathbf{Y}^{[n_a L_a, n_a S_a]} \cdot \mathbf{Y}^{[n_b L_b, n_b S_b]} \right)$$

$$\times \left(\mathbf{Y}^{[n_c L_c, n_c S_c]} \cdot \mathbf{Y}^{[n_d L_d, n_d S_d]} \right) \mathrm{d}\phi$$

$$= \frac{\pi F}{2} \sum_{n_a..n_d = \pm 1} e^{i \frac{\pi}{4}(n_a S_a + n_b S_b + n_c S_c + n_d S_d - K)}$$

$$\times \delta_{n_a S_a, -n_b S_b} \delta_{n_c S_c, -n_d S_d} \delta_{0, n_a L + n_b L_b + n_c L_c + n_d L_d}$$

$$= \frac{\pi F}{2} \sum_{n_a..n_d = \pm 1} e^{-i \frac{\pi}{4} K} \delta_{n_a S_a, -n_b S_b} \delta_{n_c S_c, -n_d S_d}$$

$$\times \delta_{0, n_a L + n_b L_b + n_c L_c + n_d L_d}, \tag{B8}$$

where the azimuthal integral was evaluated according to the last section. Each term differs by a constant term in the exponential, $K = n_a + n_b + n_c + n_d$. In the final expression, we applied the S Kronecker deltas to the exponential factor.

We will now simplify this expression by pairing the 16 terms with their complex conjugates (i.e., the term with a particular set of n_a, n_b, n_c, n_d values is conjugate to the $-n_a$, $-n_b$, $-n_c$, $-n_d$ term). Combining each conjugate pair, we find the general form for each of the eight resulting terms:

$$G_{n_a n_b n_c n_d} = \pi F \cos\left(\frac{\pi}{4} K\right) \delta_{n_a S_a, -n_b S_b} \delta_{n_c S_c, -n_d S_d}$$

$$\times \delta_{0, n_a L + n_b L_b + n_c L_c + n_d L_d}. \tag{B9}$$

With this definition, $O_{abcd} = G_{++++} + G_{+++-} + G_{++-+} + G_{++--} + G_{+-++} + G_{+-+-} + G_{+--+} + G_{-+++}$. Each of the eight terms has either zero, one, or two n_v parameters with $n_v = -1$ (the other variations of $\{n_v\}$ were covered by the eight complex conjugate terms). Consequently, $K = 4, 2,$ and 0 for these cases, respectively. If $K = 2$ then the cos term is 0, which immediately eliminates half the remaining terms, leaving $O_{abcd} = G_{++++} + G_{++--} + G_{+-+-} + G_{+--+}$. If $K = 0$, then the cos factor equals 1 and if $K = 4$ it equals -1. Applying this to each term, we find

$$O_{abcd} = \pi F[-\delta_{S_a, -S_b} \delta_{S_c, -S_d} \delta_{0, L_a + L_b + L_c + L_d} + \delta_{S_a, -S_b} \delta_{S_c, -S_d}$$

$$\times \delta_{0, L_a + L_b - L_c - L_d} + \delta_{S_a, S_b} \delta_{S_c, S_d} \delta_{0, L_a - L_b + L_c - L_d}$$

$$+ \delta_{S_a, S_b} \delta_{S_c, S_d} \delta_{0, L_a - L_b - L_c + L_d}], \tag{B10}$$

where we have used $\delta_{n_j S_j, n_k S_k} = \delta_{-n_j S_j, -n_k S_k}$ to ensure that the first argument in all the S Kronecker deltas is positive.

Now we find the three overlap integrals that compose $\mathsf{U}^{(\mathrm{CV})}$:

$$O_{i^* p s^* p'} = \pi F[-\delta_{S_i, -S_p} \delta_{S_s, -S_{p'}} \delta_{0, L_i + L_p + L_s + L_{p'}}$$

$$+ \delta_{S_i, -S_p} \delta_{S_s, -S_{p'}} \delta_{0, L_i + L_p - L_s - L_{p'}}$$

$$+ \delta_{S_i, S_p} \delta_{S_s, S_{p'}} \delta_{0, L_i - L_p + L_s - L_{p'}}$$

$$+ \delta_{S_i, S_p} \delta_{S_s, S_{p'}} \delta_{0, L_i - L_p - L_s + L_{p'}}], \tag{B11}$$

$$O_{i^* p' s^* p} = \pi F[-\delta_{S_i, -S_{p'}} \delta_{S_s, -S_p} \delta_{0, L_i + L_{p'} + L_s + L_p}$$

$$+ \delta_{S_i, -S_{p'}} \delta_{S_s, -S_p} \delta_{0, L_i + L_{p'} - L_s - L_p}$$

$$+ \delta_{S_i, S_{p'}} \delta_{S_s, S_p} \delta_{0, L_i - L_{p'} + L_s - L_p}$$

$$+ \delta_{S_i, S_{p'}} \delta_{S_s, S_p} \delta_{0, L_i - L_{p'} - L_s + L_p}], \tag{B12}$$

$$O_{p p' s^* i^*} = \pi F[-\delta_{S_p, -S_{p'}} \delta_{S_s, -S_i} \delta_{0, L_p + L_{p'} + L_s + L_i}$$

$$+ \delta_{S_p, -S_{p'}} \delta_{S_s, -S_i} \delta_{0, L_p + L_{p'} - L_s - L_i} + \delta_{S_p, S_{p'}} \delta_{S_s, S_i}$$

$$\times \delta_{0, L_p - L_{p'} + L_s - L_i} + \delta_{S_p, S_{p'}} \delta_{S_s, S_i} \delta_{0, L_p - L_{p'} - L_s + L_i}]. \tag{B13}$$

Notice how the same four L Kronecker deltas appear in each O, albeit in a different order each time. In the $\mathsf{U}^{(\mathrm{CV})}$ sum, we now group these L Kronecker delta terms together:

$$\mathsf{U}^{(\mathrm{CV})} = O_{i^* p s^* p'} + O_{i^* p' s^* p} + O_{p p' s^* i^*}$$

$$= \pi F\Big[- \big(\delta_{S_i, -S_p} \delta_{S_s, -S_{p'}} + \delta_{S_i, -S_{p'}} \delta_{S_s, -S_p}$$

$$+ \delta_{S_p, -S_{p'}} \delta_{S_s, -S_i} \big) \delta_{0, L_i + L_p + L_s + L_{p'}}$$

$$+ \big(\delta_{S_i, -S_p} \delta_{S_s, -S_{p'}} + \delta_{S_i, S_{p'}} \delta_{S_s, S_p} + \delta_{S_p, S_{p'}} \delta_{S_s, S_i} \big)$$

$$\times \delta_{0, L_i + L_p - L_s - L_{p'}}$$

$$+ \big(\delta_{S_i, S_p} \delta_{S_s, S_{p'}} + \delta_{S_i, S_{p'}} \delta_{S_s, S_p} + \delta_{S_p, -S_{p'}} \delta_{S_s, -S_i} \big)$$

$$\times \delta_{0, L_i - L_p + L_s - L_{p'}}$$

$$+ \big(\delta_{S_i, S_p} \delta_{S_s, S_{p'}} + \delta_{S_i, -S_{p'}} \delta_{S_s, -S_p} + \delta_{S_p, S_{p'}} \delta_{S_s, S_i} \big)$$

$$\times \delta_{0, L_i - L_p - L_s + L_{p'}} \Big]. \tag{B14}$$

The following identity will be used to considerably simplify the expression for $\mathsf{U}^{(\mathrm{CV})}$:

$$\delta_{S_a, q_1 S_c} \delta_{S_b, q_1 S_d} + \delta_{S_a, q_2 S_d} \delta_{S_b, q_2 S_c} + \delta_{S_a, -q_1 q_2 S_b} \delta_{S_c, -q_1 q_2 S_d}$$

$$= 2 \delta_{S_b + q_1 q_2 S_a, q_2 S_c + q_1 S_d}, \tag{B15}$$

where $q_k = \pm 1$. While we omit a detailed proof, the identity's validity can be understood by considering the three possible values of either of the arguments of the Kronecker delta on the RHS, -2, 0, or 2. For both delta arguments to be 2 or both arguments to be -2, all the terms in both arguments must be equal. The first two terms on the LHS sum to two if all the terms

Table 4.   Selection Rules for the CV Modes

Rule	L	S	Amplitude
1&2	$L_p + L_{p'} = \pm(L_s + L_i)$	$S_p + S_{p'} = \pm(S_s + S_i)$	$\pm 2\pi F$
3&4	$L_p - L_{p'} = \pm(L_s - L_i)$	$S_p - S_{p'} = \pm(S_s - S_i)$	$2\pi F$

on the RHS are equal, thereby covering these cases. The third term and one of the other first two terms on the LHS cover the remaining case, in which both RHS delta arguments are zero.

Applying this identity to $\mathsf{U}^{(CV)}$ four times and reordering the arguments of the Kronecker deltas, we find

$$\mathsf{U}^{(CV)} = 2\pi F$$

$$\times [-\delta_{S_s + S_i, -(S_p + S_{p'})} \delta_{L_s + L_i, -(L_p + L_{p'})}$$

$$+ \delta_{S_s - S_i, S_p - S_{p'}} \delta_{L_s - L_i, L_p - L_{p'}}$$

$$+ \delta_{S_s + S_i, S_p + S_{p'}} \delta_{L_s + L_i, L_p + L_{p'}}$$

$$+ \delta_{S_s - S_i, -(S_p - S_{p'})} \delta_{L_s - L_i, -(L_p - L_{p'})}]. \qquad \textbf{(B16)}$$

These four terms correspond to four selection rules, each of which has an L sub-rule and S sub-rule. These are summarized in Table 4.

In Table 4, either the top or bottom symbol of $\pm$ and $\mp$ should be taken consistently throughout each rule. More than one rule can hold true simultaneously, and their amplitudes should be added to find U, the total process amplitude.

In Fig. 3 in Section 4, we compile the amplitudes $(\times 2\pi F)$ for all distinguishable processes. We consider only the simplest case, one in which all four fields are chosen from the set of four CV modes defined by having the same value of $|L| = |l|$. As an example of this, we will identify the relevant modes for $|L| = 1$ (i.e., TM, TE, etc.), but the results hold for all $|L|$. The labels p and p' are interchangeable without changing the physical process, likewise for output fields s and i. In accordance with this, we simply label the input and output mode indices by subscripts 1 and 2. With this in mind, in our scenario, there are 10 physically distinct mode combinations for the pump modes and the same for the output modes. (In combinatorial multiset notation, $\left(\!\binom{n}{k}\!\right) = 10$ for $n = 4$ modes and $k = 2$ input/output fields.) It follows that there are $10 \times 10 = 100$ potential distinct FWM processes in total.

3. Process Amplitudes for the Total Angular Momentum Modes

We can use the results of the previous two sections to find selection rules for the TAM mode basis, i.e., the modes with definite j that are simultaneously fiber eigenmodes. We categorize the potential processes into three cases, which we treat separately in the following subsections. In each, we find $\mathsf{U}^{(TAM)}$, the process amplitude. The results are summarized in Table 5.

Case 1: interconversion of $j = 0$ modes. First we consider interconversion between the two $j = 0$ modes, $\mathbf{Z}^{[-0]}$ and $\mathbf{Z}^{[+0]}$ (i.e., the TE and TM modes, respectively). All the potential processes will trivially conserve j since it is equal

Table 5.   Summary of Allowed FWM Processes between TAM Modes

Case	Process Type	Allowed Processes	Amplitude, $\mathsf{U}^{(TAM)}$
1	$\mathbf{Z}^{[w0]} + \mathbf{Z}^{[q0]}$ $\to \mathbf{Z}^{[q0]} + \mathbf{Z}^{[q0]}$	$w = \pm, q = \pm$	$\begin{pmatrix} 2\pi F \text{ for } w \neq q \\ 6\pi F \text{ for } w = q \end{pmatrix}$
2	$\mathbf{Y}^{[s_p, s_p]} + \mathbf{Y}^{[s_{p'}, s_{p'}]}$ $\to \mathbf{Y}^{[s_i, s_i]} + \mathbf{Y}^{[s_s, s_s]}$	$s_p + s_{p'} = s_i + s_s$	$4\pi F$
3b	$\mathbf{Z}^{[w0]} + \mathbf{Z}^{[w0]}$ $\to \mathbf{Y}^{[q,q]} + \mathbf{Y}^{[-q,-q]}$	$w = \pm, q = \pm 1$	$4\pi F$
3b	$\mathbf{Y}^{[q,q]} + \mathbf{Y}^{[-q,-q]}$ $\to \mathbf{Z}^{[w0]} + \mathbf{Z}^{[w0]}$	$w = \pm, q = \pm 1$	$4\pi F$
3c	$\mathbf{Z}^{[w0]} + \mathbf{Y}^{[q,q]}$ $\to \mathbf{Z}^{[w0]} + \mathbf{Y}^{[q,q]}$	$w = \pm, q = \pm 1$	$4\pi F$

to zero for every involved mode. Since these are CV modes, these cases will be governed by the corresponding selection rules and amplitudes from Eq. (B16). As in the previous section, the only disallowed processes are ones in which there is a single unpaired mode among the four modes in the process, e.g., $\text{TM} + \text{TE} \to \text{TM} + \text{TM}$. Note that this process would be allowed by TAM conservation, so this principle by itself is not the sole selection rule for the TAM basis. If all the modes are alike, $\mathsf{U}^{(TAM)} = 6\pi F$, otherwise, $\mathsf{U}^{(TAM)} = 2\pi F$.

Case 2: interconversion of $j = \pm 2$ modes. Similarly, we can consider conversion between the $j = \pm 2$ modes in the TAM basis. These are the $\mathbf{Z}^{[2]} = \mathbf{Y}^{[1,1]}$ and $\mathbf{Z}^{[-2]} = \mathbf{Y}^{[-1,-1]}$ modes. The relevant selection rules, given by Eq. (B6), are simply those that separately conserve SAM s and OAM l, $s_i + s_s = s_p + s_{p'}$ and $l_i + l_s = l_p + l_{p'}$. Since in each beam, $s = l$, one type of angular momentum conservation is automatically accompanied by the other. Additionally, the TAM will also be trivially conserved since $j = s + l$. Conversely, the only way to conserve TAM for these modes is for SAM and OAM to be conserved.

Case 3: conversion between $j = 0$ and $j = \pm 2$ modes. Last, we consider interconversion between the $j = \pm 2$ modes and the $j = 0$ modes. We describe the two $j = 0$ modes $\mathbf{Z}^{[\pm 0]}$ with a single expression that depends on a single parameter, $m = \pm 1$:

$$\mathbf{Z}^{[m0]} = \mathbf{CV}^{[-m,m]} = \frac{1}{\sqrt{2}} e^{i\frac{\pi}{4}(m-1)} \left(\mathbf{Y}^{[1,-1]} + m\mathbf{Y}^{[-1,1]} \right).$$

$$\textbf{(B17)}$$

Since each overlap integral O is linear in a given beam's mode, if that beam is in a $\mathbf{Z}$ mode, the number of terms in $\mathsf{U}^{(TAM)}$ will double. Each term will correspond to a process amplitude $\mathsf{U}^{(Y)}$ for the $\mathbf{Y}$ modes in Eq. (B17). (We will show how this works below). We will derive the selection rules for the TAM modes using the selection rules of the constituent $\mathbf{Y}$ modes. Key will be the fact that each field q in a $\mathbf{Z}$ mode will have anti-aligned SAM and OAM, $s_q = -l_q$, whereas they will be aligned for each beam in a $\mathbf{Y}$ mode, $s_q = l_q$. We now separately consider the sub-cases in which one, two, or three of the beams are in $\mathbf{Z}$ modes.

Sub-case 3a: one beam in a $j = 0$ mode. We start with the case of a sole beam in a $\mathbf{Z}$ mode, say the idler beam. By linearity, the superposition of two $\mathbf{Y}$ modes in the $\mathbf{Z}$ factor leads to two terms in the TAM process amplitude:

$$\mathsf{U}^{(\mathrm{TAM})} = \frac{1}{\sqrt{2}} e^{i\frac{\pi}{4}(m_i-1)} \left(\mathsf{U}^{(Y)}_{+spp'} + m_i \mathsf{U}^{(Y)}_{-spp'} \right). \quad \textbf{(B18)}$$

Here, $\mathsf{U}^{(Y)}_{ispp'}$ is the process amplitude for four fields in **Y** modes [i.e., Eq. (B6)], where if the field subscript $v = i, s, p, p'$ is replaced by $n_v = \pm 1$, it indicates that field v is in mode $\mathbf{Y}^{[n_v, -n_v]}$. Each $\mathsf{U}^{(Y)}_{ispp'}$ term is non-zero only if it satisfies the standard **Y** mode selection rules, in which case $\mathsf{U}^{(Y)}_{ispp'} = 4\pi F$, regardless of which four **Y** modes are involved. At least one term must be an allowed process for $\mathsf{U}^{(\mathrm{TAM})}$ to be non-zero. In the current case, the **Y** rules become $n_i + s_s = s_p + s_{p'}$ and $-n_i + l_s = l_p + l_{p'}$ for each of the two $\mathsf{U}^{(Y)}_{n_i spp'}$ terms, where $n_i = \pm 1$ sets the term considered. However, since for all the other fields $s_j = l_j$ (i.e., modes $j = i, s, p$, are in $\mathbf{Y}^{[\pm n_j, \pm n_j]}$), we have $n_i + s_s = s_p + s_{p'}$ and $-n_i + s_s = s_p + s_{p'}$. Subtracting the two expressions, we are left with $n_i = 0$, which contradicts $n_i = \pm 1$. Consequently, neither term is allowed, and $\mathsf{U}^{(\mathrm{TAM})}$ is always zero in the current case. In other words, a process involving a single **Z** mode is not allowed.

Sub-case 3b: both input beams or both output beams in $j = 0$ modes. We now move on to the case with two input beams in **Z** modes. The reasoning will be similar, but now we must also consider the relative amplitudes of the terms, since they could cancel each other. Though we shall not describe it explicitly, the case with two output beams in **Z** modes follows the same selection rules. Now that there are two **Z** modes, there are four terms in the process amplitude:

$$\mathsf{U}^{(\mathrm{TAM})} = \frac{1}{2} e^{i\frac{\pi}{4}(m_i+m_s-2)} (\mathsf{U}^{(Y)}_{++pp'} + m_i \mathsf{U}^{(Y)}_{-+pp'}$$

$$+ m_s \mathsf{U}^{(Y)}_{+-pp'} + m_i m_s \mathsf{U}^{(Y)}_{--pp'})$$

$$= \frac{1}{2} e^{i\frac{\pi}{4}(m_i+m_s-2)} \left(m_i \mathsf{U}^{(Y)}_{-+pp'} + m_s \mathsf{U}^{(Y)}_{+-pp'} \right)$$

$$= \frac{1}{2} e^{i\frac{\pi}{4}(m_i+m_s-2)} 4\pi F (m_i + m_s), \quad \textbf{(B19)}$$

where we shall now explain the steps between the lines. Analogous to the last case, each term must satisfy $n_i + n_s = s_p + s_{p'}$ and $-n_i - n_s = s_p + s_{p'}$. Adding and subtracting these, we are left with $n_i = -n_s$ and $s_p = -s_{p'}$. The latter must be true for the whole process. The former sets which terms are non-zero. The second line above is the remaining terms, the cross-terms (e.g., $n_i = 1$, $n_s = -1$) between the **Z** mode superpositions. The process amplitudes are equal, $\mathsf{U}^{(Y)}_{-+pp'} = \mathsf{U}^{(Y)}_{+-pp'} = 4\pi F$, giving the third line above. Consequently, in this sub-case, $\mathsf{U}^{(\mathrm{TAM})}$ is non-zero only if $m_i = m_s$. In other words, the two **Z** modes must be the same (e.g., $m_i = m_s$) and the **Y** modes must be opposite (e.g., $s_p = -s_{p'}$). The total process amplitude is $\mathsf{U}^{(\mathrm{TAM})} = \pm 4\pi F e^{i\frac{\pi}{4}(\pm 2-2)} = 4\pi F$.

Sub-case 3c: one input beam and one output beam in $j = 0$ modes. The next case, where one input beam and one output beam are in a **Z** mode, follows reasoning similar to the last. And so, $n_i + s_s = n_p + s_{p'}$ and $-n_i + s_s = -n_p + s_{p'}$ must be satisfied for a term to be non-zero. This leads to $s_s = s_{p'}$ and $n_i = n_{p'}$. With this,

$\mathsf{U}^{(\mathrm{TAM})} = \frac{1}{2} e^{i\frac{\pi}{4}(m_i+m_s-2)} 4\pi F(1 + m_i m_s)$. Thus, $\mathsf{U}^{(\mathrm{TAM})}$ is non-zero only if $m_i = m_s$, which means the input beam is in the same **Z** mode as the pump, and the remaining input and pump beams are in the same **Y** mode (e.g., $s_s = s_{p'}$). Again, the total process amplitude is $\mathsf{U}^{(\mathrm{TAM})} = 4\pi F$.

Sub-case 3d: three beams in $j = 0$ modes. The last case, three of the four beams in **Z** modes, is relatively simple. There will be six terms in $\mathsf{U}^{(\mathrm{TAM})}$, each of which must satisfy $n_i + n_s = n_p + s_{p'}$ and $-n_i - n_s = -n_p + s_{p'}$. Combining these equations leads to the contradiction $s_{p'} = 0$. Consequently, no such process is possible.

All the allowed processes and their relative amplitudes are listed in Table 5.

REFERENCES

1. N. Bozinovic, Y. Yue, Y. Ren, M. Tur, P. Kristensen, H. Huang, A. Willner, and S. Ramachandran, "Terabit-scale orbital angular momentum mode division multiplexing in fibers," Science **340**, 1545–1548 (2013).

2. J. Liu, S.-M. Li, L. Zhu, A.-D. Wang, S. Chen, C. Klitis, C. Du, Q. Mo, M. Sorel, S.-Y. Yu, X.-L. Cai, and J. Wang, "Direct fiber vector eigenmode multiplexing transmission seeded by integrated optical vortex emitters," Light Sci. Appl. **7**, 17148 (2018).

3. W. Qiao, T. Lei, Z. Wu, S. Gao, Z. Li, and X. Yuan, "Approach to multiplexing fiber communication with cylindrical vector beams," Opt. Lett. **42**, 2579–2582 (2017).

4. J. Li, J. Zhang, F. Li, X. Huang, S. Gao, and Z. Li, "DD-OFDM transmission over few-mode fiber based on direct vector mode multiplexing," Opt. Express **26**, 18749–18757 (2018).

5. G. Vallone, V. D'Ambrosio, A. Sponselli, S. Slussarenko, L. Marrucci, F. Sciarrino, and P. Villoresi, "Free-space quantum key distribution by rotation-invariant twisted photons," Phys. Rev. Lett. **113**, 060503 (2014).

6. R. Dorn, S. Quabis, and G. Leuchs, "Sharper focus for a radially polarized light beam," Phys. Rev. Lett. **91**, 233901 (2003).

7. P. Mitra and J. Stark, "Nonlinear limits to the information capacity of optical fibre communications," Nature **411**, 1027–1030 (2001).

8. Q. Lin and G. P. Agrawal, "Vector theory of four-wave mixing: polarization effects in fiber-optic parametric amplifiers," J. Opt. Soc. Am. B **21**, 1216–1224 (2004).

9. K. Garay-Palmett, D. Cruz-Delgado, F. Dominguez-Serna, E. Ortiz-Ricardo, J. Monroy-Ruz, H. Cruz-Ramirez, R. Ramirez-Alarcon, and A. B. U'Ren, "Photon-pair generation by intermodal spontaneous four-wave mixing in birefringent, weakly guiding optical fibers," Phys. Rev. A **93**, 033810 (2016).

10. G. Agrawal, *Nonlinear Fiber Optics, Electronics & Electrical* (Elsevier, 2007).

11. H. Pourbeyram and A. Mafi, "Photon pair generation in multimode optical fibers via intermodal phase matching," Phys. Rev. A **94**, 023815 (2016).

12. E. Nazemosadat, H. Pourbeyram, and A. Mafi, "Phase matching for spontaneous frequency conversion via four-wave mixing in graded-index multimode optical fibers," J. Opt. Soc. Am. B **33**, 144–150 (2016).

13. R. Jauregui and J. P. Torres, "On the use of structured light in nonlinear optics studies of the symmetry group of a crystal," Sci. Rep. **6**, 20906 (2016).

14. R. Saaltink, L. Giner, R. Boyd, E. Karimi, and J. Lundeen, "Super-critical phasematching for photon pair generation in structured light modes," Opt. Express **24**, 24495–24508 (2016).

15. J. Arlt, K. Dholakia, L. Allen, and M. Padgett, "Efficiency of second-harmonic generation with Bessel beams," Phys. Rev. A **60**, 2438–2441 (1999).

16. A. W. Snyder and J. Love, *Optical Waveguide Theory*, 1st ed. (Springer, 1983), Chap. 14, pp. 304–305.

17. S. Chen and J. Wang, "Theoretical analyses on orbital angular momentum modes in conventional graded-index multimode fibre," Sci. Rep. **7**, 3990 (2017).

18. Q. Zhan, "Cylindrical vector beams: from mathematical concepts to applications," Adv. Opt. Photonics **1**, 1–57 (2009).

19. L. Allen, M. W. Beijersbergen, R. J. C. Spreeuw, and J. P. Woerdman, "Orbital angular momentum of light and the transformation of Laguerre-Gaussian laser modes," Phys. Rev. A **45**, 8185 (1992).

20. P. Gregg, M. Mirhosseini, A. Rubano, L. Marrucci, E. Karimi, R. Boyd, and S. Ramachandran, "Q-plates as higher order polarization controllers for orbital angular momentum modes of fiber," Opt. Lett. **40**, 1729–1732 (2015).

21. R. W. Boyd, *Nonlinear Optics*, 3rd ed. (Academic, 2008).

22. R. Fickler, R. Lapkiewicz, W. N. Plick, M. Krenn, C. Schaeff, S. Ramelow, and A. Zeilinger, "Quantum entanglement of high angular momenta," Science **338**, 640–643 (2012).

23. P. G. Kwiat, K. Mattle, H. Weinfurter, A. Zeilinger, A. V. Sergienko, and Y. Shih, "New high-intensity source of polarization-entangled photon pairs," Phys. Rev. Lett. **75**, 4337–4341 (1995).

24. O. Cohen, J. S. Lundeen, B. J. Smith, G. Puentes, P. J. Mosley, and I. A. Walmsley, "Tailored photon-pair generation in optical fibers," Phys. Rev. Lett. **102**, 123603 (2009).

25. B. Ndagano, I. Nape, M. Cox, C. Rosales-Guzman, and A. Forbes, "Creation and detection of vector vortex modes for classical and quantum communication," J. Lightwave Technol. **36**, 292–301 (2017).

26. L. Allen, S. Barnett, and M. Padgett, *Optical Angular Momentum, Optics & Optoelectronics* (Taylor & Francis, 2003).

27. D. Andrews and M. Babiker, *The Angular Momentum of Light* (Cambridge University, 2013).